

Machine learning supported annealing for prediction of grand canonical crystal structures

Yannick Couzinié^{1,2,*} Yuya Seki^{3,4} Yusuke Nishiya^{1,2} Hirofumi Nishi^{1,2}
Taichi Kosugi^{1,2} Shu Tanaka^{4,5,6,7} and Yu-ichiro Matsushita^{1,2,8}

¹*Department of Physics, The University of Tokyo Hongo, Bunkyo-ku, Tokyo, Japan.*

²*Quemix Inc., Taiyo Life Nihombashi Building, 2-11-2, Nihombashi Chuo-ku, Tokyo, Japan*

³*Graduate School of Science and Technology, Keio University,
3-14-1 Hiyoshi, Kohoku-ku, Yokohama, Kanagawa, Japan*

⁴*Keio University Sustainable Quantum Artificial Intelligence Center (KSQAIC),
Keio University, 2-15-45 Mita, Minato-ku, Tokyo, Japan*

⁵*Department of Applied Physics and Physico-Informatics, Keio University,
3-14-1 Hiyoshi, Kohoku-ku, Yokohama, Kanagawa, Japan*

⁶*Human Biology-Microbiome-Quantum Research Center (WPI-Bio2Q),
Keio University, 2-15-45 Mita, Minato-ku, Tokyo,*

⁷*Green Computing Systems Research Organization (GCS),
Waseda University, 162-0042 Wasedamachi, Shinjuku-ku, Tokyo, Japan*

⁸*Quantum Material and Applications Research Center,*

National Institutes for Quantum Science and Technology (QST), 2-12-1, Ookayama, Meguro-ku, Tokyo, Japan

(Dated: August 8, 2024)

This study investigates the application of Factorization Machines with Quantum Annealing (FMQA) to address the crystal structure problem (CSP) in materials science. FMQA is a black-box optimization algorithm that combines machine learning with annealing machines to find samples to a black-box function that minimize a given loss. The CSP involves determining the optimal arrangement of atoms in a material based on its chemical composition, a critical challenge in materials science. We explore FMQA's ability to efficiently sample optimal crystal configurations by setting the loss function to the energy of the crystal configuration as given by a predefined interatomic potential. Further we investigate how well the energies of the various metastable configurations, or local minima of the potential, are learned by the algorithm. Our investigation reveals FMQA's potential in quick ground state sampling and in recovering relational order between local minima.

I. INTRODUCTION

Solving the crystal structure problem (CSP) from chemical composition remains an enduring challenge in materials science, demanding innovative methodologies to overcome the exponential growth of potential structures as the system size increases [1]. Various approaches on classical computers have been developed [2], e.g. random search [3–6], simulated annealing (SA) [7–9], minima hopping [10, 11], evolutionary algorithms [12–15] and particle swarm optimization [16, 17]. Various software suites such as USPEX [18, 19], CALYPSO [16, 20, 21], and CrySPY [22] are used in standard approaches to the CSP. Being on classical hardware, these algorithms do not manage to compute large scale structures. With the continually increasing computational capacity of quantum computers, there is a need to develop efficient algorithms to solve the CSP that is compatible with quantum hardware.

In recent years, the use of quantum computers has attracted a great deal of attention as a means of searching for globally optimal solutions [23–29]. Quantum computers are characterized by their ability to escape from

locally stable solutions and accelerate the search for globally optimal solutions by utilizing the quantum tunneling effect [26, 30] and the superposition of states to concurrently evaluate a large state space [31]. Quantum annealing (QA) machines [23, 32–35] and gate-based quantum computers [31] are the two main current architectures in development. Exhaustive structure search schemes using gate-based quantum computers [36–38], quantum annealers and the equivalent Ising machines [39–43] have recently been proposed.

Using the encoding proposed in [40] it is possible to encode the local interactions of any potential with a hard cutoff into a quadratic unconstrained binary optimization (QUBO) or higher order unconstrained binary optimization (HUBO) problem by discretizing the simulation cell. Optimizing the structure of ionically bonded crystals can then be described as a QUBO problem (see [39]) and that of covalently bounded crystals can be described by a third-order HUBO problem (see [40]). When it comes to non-crystalline phases of covalently bounded materials or metals, more accurate potentials such as bond-order [44, 45], machine learned [46] or embedded atom method (EAM) based potentials [47, 48] are needed. In these cases the order of the HUBO is generally equal to the amount of neighbouring lattice sites inside the cutoff radius of the respective potential.

Current Ising machines [49] such as quantum anneal-

* couzinie.y.aa@m.titech.ac.jp

ing hardware [35], or classical annealers (e.g. [50]) usually focus on the solving of QUBO problems. There are exceptions for higher order such as the QAOA algorithm [51] or simulated bifurcation machines [52], but performance in these cases still suffer from the quickly increasing number of non-zero interactions. It is possible to reduce HUBO problems to QUBO problems through usual quadratization techniques [53], but these usually add a number of auxiliary bits in the same order of the number of removed non-zero interaction terms and produce QUBOs which are not implementable on current hardware.

Thus, modern accurate interatomic potentials require high orders of interactions while currently constructed hardware is optimized for the quadratic case. We fill this gap by only considering the total energy returned by the potential instead of the sum of local interactions. This makes it possible to use black-box optimization schemes, which iteratively find more optimal inputs (i.e. the structures) to the black-box function (the potential). In particular, this also opens the possibility to use density functional theory [54] as a source for total energy values.

Various approaches exist to perform materials discovery using black-box optimization [55]. We focus on the ones combining machine learning principles with quantum annealers [56–59], and in particular on Factorization Machines with Quantum Annealing (FMQA) or Factorization Machines with Annealing (FMA) if performed on classical devices [56, 60, 61]. FMQA has been successfully applied for metamaterials discovery [55, 56] and thus seems particularly apt for an application to the CSP. FMQA iteratively learns a QUBO representation to accurately map structures to their black-box calculated energy.

As a QUBO only contains second-order interaction information, we are effectively learning a pairwise interaction representation for the CSP. It is generally known that more complicated materials, e.g. metals, cannot be described by pairwise interactions [62, 63]. Thus, we cannot expect our FMA approach to produce physically meaningful QUBOs for the whole spectrum as was the case for the original encoding in [40]. Instead, as more and more low energy states are added to the database a second-order approximation of the ground state and its surrounding states is constructed.

The two main questions we seek to answer thus in this publication are

(Q1) Can we use FMA to sample ground state configurations?

(Q2) How much information about the non-ground state local minima do the learned QUBOs contain?

To preempt the conclusion our findings are that the algorithm can be used to efficiently sample ground state configurations for complicated potentials such as the EAM and that we can quickly infer parts of the relational order of local minima, while reproducing the actual energy levels requires more intense calculations.

The rest of the paper is structured as follows. In Section II we give a detailed overview of our calculation methods and the materials and potentials we considered. In Section III we present FMA calculation results, showing that we can reproduce the ground state (Q1) for complicated potentials and Section IV discusses the quality of the spectrum of local minima produced by our approach (Q2). We end by summarising the results in Section V.

II. METHODS

In Section II A we define the functional form of our factorization machine, in Section II B the parameter optimization flow we use to produce ground state configurations and learn good factorization machine parameters. In Section II C we discuss the two main calculation paradigms we use by accounting or not for symmetry. We end the section by discussing the three systems and their potentials we use, a Krypton Lennard-Jones Cluster (Section II D), which is a pairwise potential and thus exactly learnable by our algorithm. We then consider a Silicon Stillinger-Weber system (Section II E) which is a three-body potential and thus the simplest potential that is not exactly learnable anymore. Finally, we consider a CrFe alloy with an EAM potential (Section II F) which provides a functionalized approximation for the electron density and thus mimics first principles calculations while keeping the costs low.

A. Encoding

Consider a unit cell that is spanned by a given basis $\{\vec{a}_i\}$ with periodic boundary conditions along a chosen set of basis vectors and a set of atom species \mathcal{S} . We look at a set of N lattice points X in this unit cell generated by partitioning each basis vectors into g points and forming the corresponding lattice. The lattice points have the form $\sum_i \frac{k_i}{g} \vec{a}_i$ where $k_i \in \{0, \dots, g-1\}$. Consider a set b_x^s of binary variables that we define such that if $b_x^s = 1$ there is an atom of species $s \in \mathcal{S}$ on $x \in X$. In [40] a method was introduced that could encode any interatomic potential with hard cutoff into a HUBO of the form

$$\begin{aligned}
 H &= \sum_{\substack{x \in X \\ s \in \mathcal{S}}} V_1^s(x) b_x^s \\
 &+ \frac{1}{2!} \sum'_{\substack{x_1, x_2 \in X \\ s_1, s_2 \in \mathcal{S}}} V_2^{s_1, s_2}(x_1, x_2) b_{x_1}^{s_1} b_{x_2}^{s_2} + \dots \\
 &+ \frac{1}{M!} \sum'_{\substack{x_1, \dots, x_M \in X \\ s_1, \dots, s_M \in \mathcal{S}}} V_M^{s_1, \dots, s_M}(x_1, \dots, x_M) b_{x_1}^{s_1} \dots b_{x_M}^{s_M},
 \end{aligned} \tag{1}$$

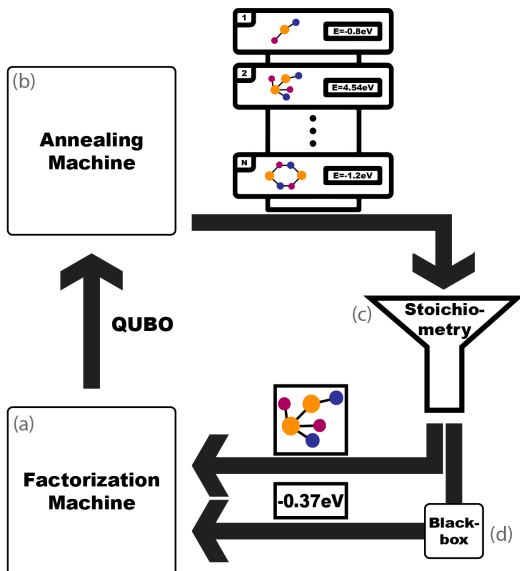


FIG. 1: The flowchart of our FMA algorithm. The factorization machine (a) is instantiated with an initial dataset and outputs an initial QUBO. The annealing machine (b) samples a set number of samples from the QUBO. Configurations that do not satisfy the stoichiometric constraints are filtered by the stoichiometry filter (c). The remaining (lowest energy) configurations are evaluated with the black-box function (d) and added to the dataset where the cycle repeats starting with the factorization machine (a). This cycle is repeated for the preset amount of iterations.

with an appropriately chosen M . Using FMA we will approximate this encoding as Factorization machines [64], which are functions of the form

$$f(\mathbf{b}) = \sum_{s \in \mathcal{S}} \sum_{i=1}^{|\mathcal{X}|} w_{is} b_i^s + \sum_{s_1, s_2 \in \mathcal{S}} \sum_{i < j} \sum_{n=1}^k v_{is_1 n} v_{js_2 n} b_i^{s_1} b_j^{s_2}, \quad (2)$$

where k is a hyperparameter that governs how many parameters (i.e. the set $\{w_i, v_{isn}\}$) there are in the model and finding binary strings that minimize $f(\mathbf{b})$ is a QUBO problem. The goal of our FMA approach is finding the parameters such that the optimal solution to the QUBO problem is the ground state and ideally local minima correspond to physical local minima.

B. FMA setup

The general outline of the FMA iteration is given in Fig. 1. We start the FMA calculations by generating an initial dataset comprised of a preset number of configurations of a system dependent number of atoms on the lattice together with their respective energies. These configurations are randomly generated in a way that no

two atoms collide and such that the stoichiometric constraints of the problem are respected. The stoichiometric constraints here refer to the relative density of the atoms, e.g. if we want to optimize for CrFe configurations we only generate initial configurations that have the same amount of Cr and Fe atoms. We add a penalty to the energy proportional to how badly the stoichiometric constraints are broken where the strength of the penalty $P = 20\text{eV}$ is another hyperparameter.

At the sampling stage, we sample 1000 samples from the resulting QUBO using simulated annealing [65] adding a penalty term to the QUBO that penalises atom collisions, i.e. the interaction term between $b_i^{s_1}$ and $b_i^{s_2}$ for two different species s_1, s_2 on the same lattice site is increased by P . We use the same geometric schedule and bit-flip neighbourhood as in [40] with maximum temperature 1, minimum temperature 0.001 and 5 schedule steps. The temperature range is not problem specific as we normalize the QUBO resulting from the factorization machine so that individual interaction terms J_{ij} are limited to $[-1, 1]$. After filtering out the configurations that break the stoichiometric constraints we transform the binary vectors into configurations readable by the atomic simulation environment (ASE, [66]), calculate the energies using a predefined potential (this is the black-box), add the lowest energy 5 configurations to the dataset and start the loop again. The final output after 50 iterations is the lowest-energy configuration in the dataset.

C. Accounting for symmetries

In this paper we only consider systems that have periodic boundary conditions along all three basis directions. Thus, for any particular local minimum energy there are multiple configurations that are translated or rotated versions of another. We call calculations with this encoding *unconstrained*. To account for the translational symmetry we also perform a *Fixed Zero* calculation in which we fix an atom on the origin, by setting the corresponding binary variable to 1 for one of the species and 0 for the others, reducing the amount of binary variables in the problem by $|\mathcal{S}|$.

D. Krypton system

For the calculation of the potential functions we rely on the Open Knowledgebase of Interatomic Models (OpenKIM) [67]. In particular we will look at a three dimensional cubic unit cell of side length 5.653\AA with the Lennard-Jones (LJ) potential parameters due to Bernades for Krypton [67–71]. We discretize the unit cell into an equipartitioned lattice of 4^3 nodes by setting $g = 4$. The ground state is given by the FCC configuration and thus encodable on the lattice. The initial dataset consists of all 64 single atom Kr_1 and all 2016 two atom Kr_2 configurations on the lattice. For the

fixed zero system the initial dataset not only contains the 63 Kr₂ configurations but also all 1953 three atom Kr₃ configurations. The energy of the FCC configuration is -0.119eV/atom which we take as the zero energy. We will simply refer to this system as the Krypton system.

E. Silicon system

We optimize the configuration of pure silicon governed by the Stillinger-Weber potential parametrisation due to Balamane, Halicioglu and Tiller [67, 69, 70, 72–76]. The unit cell is cubic with side length 5.44\AA which we again discretize into 4^3 nodes by setting $g = 4$. The well-known Si₈ crystal ground state configuration is then encodable on the lattice. The energy of the ground state is -4.630eV/atom which we set as the 0 energy for this system. The initial dataset consists of 8000 randomly sampled Si₈ configurations on the lattice.

F. CrFe system

We optimize the configuration of a chrome-iron alloy governed by the modified embedded atom-method potential parametrisation due to Lee, Shim and Park [69, 70, 77–79]. We use an orthorhombic unit cell with side length 2.92310\AA , 3.88108\AA , 4.02297\AA found on Materials Project [80][81]. We discretize this unit cell again into 4^3 nodes by setting $g = 4$, so that the problem has $2 \cdot 64 = 128$ bits as we have two atom species. The reference structure is a Cr₂Fe₂ configuration that has -4.088eV/atom as the ground state energy which we set as the 0 energy. Our initial datasets consist of 8000 randomly sampled Cr₂Fe₂ configurations on the lattice.

III. FINDING THE GROUND STATE

A. Setup

We perform calculations for two sets of parameters, one that we call the *quick settings* and one we call *accurate settings*. The idea is that to find optimal crystal configurations speed is more important than having accurate QUBOs. To investigate how well we can approximate our HUBO as a QUBO we will use the more time intensive accurate settings.

In both settings we initialize the factorization machines with random weight and use the AdamW method to optimize them. In the quick settings we set $k = 20$ use a learning rate of 0.08 and learn for 10 epochs for a total of 50 iterations. This calculation aims at quickly sampling the iteratively learned QUBO to find the ground state.

In the accurate settings we set $k = 70$ for the Krypton and Silicon systems and $k = 140$ for the CrFe system. We set the learning rate to 0.01 and learn for 2500 epochs and a total of 20 iterations. We determined these settings

System	Quick		Accurate	
	Count	Iterations	Count	Iterations
Krypton	30	1.7 ± 0.23	30	1 ± 0
Si	30	17.0 ± 0.36	30	7.0 ± 0.57
CrFe	24	17.9 ± 2.11	28	11.9 ± 0.58

TABLE I: The number of runs (of a total of 30) where the ground state is found during one of the FMA iterations for the unconstrained system and the average amount of iterations with standard deviation for the first iteration at which the ground state was sampled. The Krypton values for the accurate settings are 1 ± 0 as the parameters are chosen such that the exact representation is learned in one iteration.

by increasing the epoch number, and k , and decreasing the learning rate until the Krypton system (whose potential is pairwise, and thus perfectly representable as a QUBO) was perfectly learned by the FMA algorithm in one iteration.

To account for the randomness in the initial dataset and FMA initialization we perform 30 independent FMA runs for each system and extract the QUBO producing the lowest energy sample from each run. Note that the *learned energy* (i.e. the energy as given by the QUBO) that gets sampled does not match the *reference energy* (i.e. the energy as calculated by the black-box potential function), and we determine the lowest energy configuration by considering its reference energy and not its learned energy. We use the word *learned* to refer to the results as produced by the FMA algorithm and *reference* to refer to the true values as given by the potential function. To judge how good the algorithm is at finding the reference ground state we look at how many runs return the reference ground state and how many iterations it takes on average to recover the reference ground state. We do this separately for the unconstrained (Table I) and fixed zero (Table II) systems.

B. Results & Discussion

We see in Table I that for the unconstrained system we are able to sample the reference ground state in the quick settings in all iterations for the Krypton and Si systems and in 24 of 30 iterations for the CrFe system, which is improved to 28 in the accurate settings. We also see that, as expected, the accurate settings requires less iterations until the reference ground state is sampled, which likely stems from the higher number of performed epochs leading to a more accurate second order approximation of the dataset and thus to more high-quality annealing sample. For the fixed zero calculations results (Table II) we see that for the quick settings in the Krypton system we only find the ground state for 25 iterations taking 10.7 iterations on average as opposed to 1.7 for the unconstrained system. For the silicon system the iteration number is

System	Count	Quick		Accurate	
		Count	Iterations	Count	Iterations
Krypton	25	10.7 \pm 1.42	30	1 \pm 0	
Si	30	18.4 \pm 1.14	25	8.3 \pm 0.95	
CrFe	0	N/A	0	N/A	

TABLE II: Same as Table I for the fixed zero system.

slightly increased and in the accurate settings we only manage to find the ground state in 25 out of 30 runs. For the CrFe system with fixed zeros we do not manage to sample the ground state in any iteration. This might be due to a local minimum consistently having a lower learned energy than the reference ground state (see for example Fig. 3 in the next section). In Fig. 2 we see the cumulative minimum over the 30 FMA runs for the quick setting. It is easily observable that the Fixed zero calculations (green) perform worse than the unconstrained ones (blue) for the non-exactly learnable systems of Si and FeCr. Further, while the average iteration to find the ground state was similar in Table II we see that unconstrained CrFe tends to have a lower cumulative minimum and quickly goes to a residual energy of around 3-4 eV and then slowly decreases while Silicon has a more linear deterioration. For the fixed zero calculations we see that CrFe slowly decreases to a non-zero residual energy, which is reflected in the fact that we do not sample the ground state while the Silicon calculation is roughly comparable to the unconstrained case. In total we see that fixing the zero gives comparable or worse performance.

It is expected that the Krypton system outperforms both the Silicon and the CrFe system at the quick settings, as the reference LJ potential is a pairwise potential and hence representable as a QUBO as done in [39, 40] and recovered for the accurate settings. Thus, if the parameter for the interaction between atoms on two sites x and y of the lattice is correctly estimated to reproduce the energy of a configuration in the dataset, it will be correctly estimated for any configuration in the dataset and should thus be correctly reflected in the learned potential. For the higher order potentials the energy contribution of a pair of atoms is much harder to estimate as the contribution in the reference potential might vary drastically depending on the surrounding configuration, e.g. the interaction between x and y depends on the angles it forms with other atoms neighbouring them.

To summarize the results, considering the unconstrained system we see that our FMQA setup is able to efficiently sample the ground state configurations of arbitrary potentials, even if multiple iterations are recommended to ensure that the ground state is found (see CrFe results in Table I). As opposed to previous findings [61], we do not see evidence that reducing the bit number necessarily has a favorable impact on the difficulty of the problem.

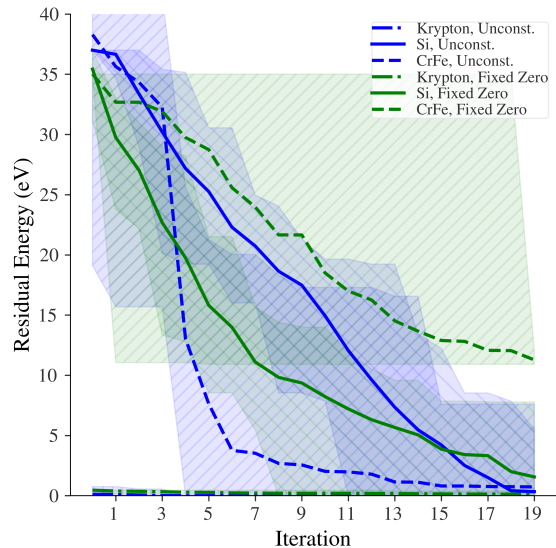


FIG. 2: Cumulative minimum over 30 FMA runs for the quick setting plotted against the iteration until which the cumulative minimum is taken. The solid, dashed and dash-dotted lines are the mean cumulative minimum and the shaded areas the corresponding minimum and maximum cumulative minimum until that iteration.

Silicon is in solid, CrFe in dashed, Krypton in dash-dotted. Unconstrained calculations are in blue and fixed zero calculations in green. Bottom-left to top-right shaded areas are for CrFe and the inverse orientation for Silicon. Horizontally dashed lines are for Krypton.

IV. REPRODUCTION OF ORDER OF LOCAL MINIMA

A. Setup

We consider the quick and accurate settings for the local minima reproduction.

We extract the set of all local minima of the reference potential represented on our lattice. We define a state on the lattice as a reference local minimum if it has an atom density of that of the reference ground state or lower, satisfies the stoichiometric constraints, has an absolute force on the atoms of 0 and if its energy is lower than 0. Note that in our encoding we provide no information on the force and thus, due to the discretization, there might be other meta-stable local minima when constraining the system to the lattice, nonetheless we only consider the force-free local minima as given by the reference potential, as these are the physical local minima.

We judge the reproduction of the reference spectrum using the relational order of the learned energy. This is because as long as the learned energy levels have the correct relational order, their reference value is not as important, as it is usually inexpensive to recalculate the energies of the local minima if they are correctly identified.

	Quick		Accurate	
	Unconstrained	Fixed Zero	Unconstrained	Fixed zero
Krypton	0.32	0.72	1	1
Si	0.32	0.44	0.26	0.45
CrFe	0.48	0.69	0.41	0.68

TABLE III: The results for the Kendall coefficient.

We do this using the Kendall rank coefficient [82] a real number between -1 and 1 . In our case, a value of 1 indicates that the learned local minima energy levels have the same order as the reference ones, and a value of -1 that the order is reversed while 0 indicates no order. Ideally, FMA would produce QUBOs that have a value of 1 .

For each set of calculation parameters we consider the iteration that produces the highest Kendall rank coefficient QUBO.

B. Results & Discussion

The results for the Kendall coefficients for the various systems are given in Table III. We see that generally the fixed zero system improves the Kendall coefficient and that the CrFe system outperforms the Silicon system. To understand this, consider that for the Silicon system we have 7056 (482) local minima and for the CrFe system we have 1856 (52) with the fixed zero system value in brackets. Since FMQA performs a quadratic approximation of the potential energy landscape around the states in the database, having fewer local minima that get sampled makes it easier to represent these accurately. This is particularly apparent for the 0.72 value of fixed zero Krypton in which only 20 local minima are considered.

The quick settings also tend to slightly outperform the accurate settings. A possible explanation is given by Fig. 3 in which the learned energy levels (blue dots) are plotted against their reference values for the quick (left) and accurate (right) settings of the CrFe fixed zero system. It is apparent that in the accurate settings, we more accurately reflect the actual energy levels of the potential. The fit is not close to chemical accuracy, which is easily explained by considering that we are approximating a many-body potential with a quadratic function. In particular this shows how well FMQA can quadratize a HUBO problem into a QUBO. The quick settings on the other hand do not represent the actual values of the energy levels well but their relational order as there is more distance between the various local minima.

Notice also, that in the shown accurate settings the ground state of the learned energies and reference energies are not equal and we can sample the ground state only because we take 1000 samples from the QUBO at every iteration. This reliance on a high sample number could be problematic if our black-box is a first principle based calculator with high computational costs.

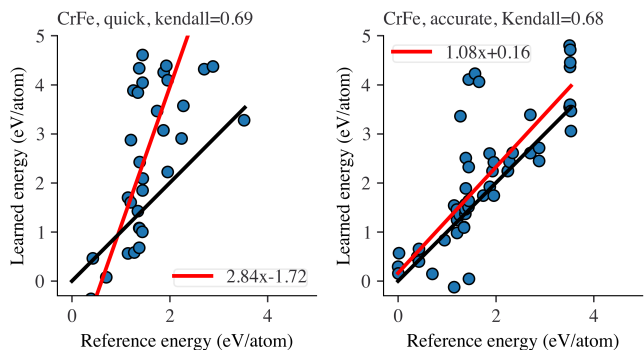


FIG. 3: Learned energy levels as blue dots for the fixed zero CrFe system for the quick settings (left) and accurate settings (right) plotted against the energy for the reference potential. The black diagonal corresponds to the reference values and the red line to a linear regression resulting in a line $2.84x - 1.72$ for the quick settings and $1.08x + 0.16$ for the accurate settings. The Kendall rank coefficient is 0.69 and 0.68 respectively.

These results hint at the possibility that to learn relational orders an exploratory learning phase such as in the quick settings is enough, and even beneficial as local minima whose reference value is close are learned with values far apart. The accurate settings lend themselves more to learn a quadratic representation of the potential.

V. CONCLUSIONS

In conclusion, this publication explores the application of Factorization Machines with Quantum Annealing (FMQA) to the crystal structure problem (CSP) in materials science. The CSP involves determining the optimal arrangement of atoms in a material based on its chemical composition. The study investigates the capability of FMQA to efficiently sample ground state configurations and reproduce the spectrum of local minima energy levels.

The results show that FMQA can be used to quickly sample ground state configurations of various potential forms including three-body Stillinger-Weber potentials and EAM potentials.

We show that using calculation settings that quickly finish the relational order between local minima is well represented in particular when accounting for translational symmetry by fixing an atom on the origin. Factorization machines are known to lend themselves well for machine learned ranking [64] this work marks a first exploration into how well the FMA algorithm can be applied on the same problem. Using more time-intensive accurate settings we further show that the local minima of a metal alloy using an EAM potential is well approximated by the quadratic QUBO matrix. While the accuracy is not enough to serve as an interatomic potential,

we have shown the potential of FMQA as a quadratization scheme for HUBO problems.

As opposed to previous findings [61], we did not observe that reducing the search space improves the quality of the results. The results in [61] are not directly applicable here, but our findings still raise the need for further investigation into the relation of search space size and FMQA performance.

There are several ways the FMQA algorithm could be improved to potentially provide more faithful approximated potentials. An obvious improvement is going to higher-order factorization machines [83, 84], though this suffers from the same problem as the higher-order encoding presented in [40] in that sampling HUBOs is not efficient on current hardware. Recently high-quality non-parametric potentials 3-body potentials have been proposed [85, 86] and so it might not be necessary to go to higher-order but rather add non-linearities for example by replacing the dot product in factorization machines with kernels [87].

The study highlights the importance of considering the nature of interatomic potentials and system complexity when applying quantum-enhanced algorithms to materials science problems. The findings contribute to the ongoing exploration of quantum computing methodologies for addressing challenges in materials discovery and

crystal structure determination.

ACKNOWLEDGMENTS

This work was supported by JSPS KAKENHI as “Grant-in-Aid for Scientific Research(A)” Grant Number 21H04553 and “Grant-in-Aid for Scientific Research(S)” JP23H05447. This paper is partially based on results obtained from a project, JPNP23003, commissioned by the New Energy and Industrial Technology Development Organization (NEDO). This work was supported by the Center of Innovations for Sustainable Quantum AI (JST Grant Number JPMJPF2221). This work was partially supported by the Council for Science, Technology, and Innovation (CSTI) through the Cross-ministerial Strategic Innovation Promotion Program (SIP), “Promoting the application of advanced quantum technology platforms to social issues” (Funding agency: QST). S. T. wishes to express their gratitude to the World Premier International Research Center Initiative (WPI), MEXT, Japan, for their support of the Human Biology-Microbiome-Quantum Research Center (Bio2Q).

The computation in this work has been done using the supercomputer provided by Supercomputer Center at the Institute for Solid State Physics at the University of Tokyo.

-
- [1] J. Maddox, Crystals from first principles, *Nature* **335**, 201 (1988).
- [2] A. R. Oganov, C. J. Pickard, Q. Zhu, and R. J. Needs, Structure prediction drives materials discovery, *Nature Reviews Materials* **4**, 331 (2019).
- [3] C. J. Pickard and R. J. Needs, High-pressure phases of silane, *Phys. Rev. Lett.* **97**, 045504 (2006).
- [4] C. J. Pickard and R. J. Needs, Structure of phase III of solid hydrogen, *Nature Physics* **3**, 473 (2007).
- [5] C. J. Pickard and R. J. Needs, Ab initio random structure searching, *Journal of Physics: Condensed Matter* **23**, 053201 (2011).
- [6] R. J. Needs and C. J. Pickard, Perspective: Role of structure prediction in materials discovery and design, *APL Materials* **4**, 053210 (2016).
- [7] L. Wille, Minimum-energy configurations of atomic clusters: new results obtained by simulated annealing, *Chemical Physics Letters* **133**, 405 (1987).
- [8] L. Wille, Simulated annealing and the topology of the potential energy surface of lennard-jones clusters, *Computational Materials Science* **17**, 551 (2000).
- [9] X. Yin and C. E. Gounaris, Search methods for inorganic materials crystal structure prediction, *Current Opinion in Chemical Engineering* **35**, 100726 (2022).
- [10] S. Goedecker, Minima hopping: An efficient search method for the global minimum of the potential energy surface of complex molecular systems, *The Journal of Chemical Physics* **120**, 9911 (2004).
- [11] M. Amsler and S. Goedecker, Crystal structure prediction using the minima hopping method, *The Journal of Chemical Physics* **133**, 224104 (2010).
- [12] T. S. Bush, C. R. A. Catlow, and P. D. Battle, Evolutionary programming techniques for predicting inorganic crystal structures, *J. Mater. Chem.* **5**, 1269 (1995).
- [13] A. R. Oganov and C. W. Glass, Crystal structure prediction using ab initio evolutionary techniques: Principles and applications, *The Journal of Chemical Physics* **124**, 244704 (2006).
- [14] A. R. Oganov, A. O. Lyakhov, and M. Valle, How evolutionary crystal structure prediction works—and why, *Accounts of Chemical Research* **44**, 227 (2011).
- [15] A. O. Lyakhov, A. R. Oganov, H. T. Stokes, and Q. Zhu, New developments in evolutionary structure prediction algorithm USPEX, *Computer Physics Communications* **184**, 1172 (2013).
- [16] Y. Wang, J. Lv, L. Zhu, and Y. Ma, Crystal structure prediction via particle-swarm optimization, *Phys. Rev. B* **82**, 094116 (2010).
- [17] Y. Zhang, H. Wang, Y. Wang, L. Zhang, and Y. Ma, Computer-assisted inverse design of inorganic electrides, *Phys. Rev. X* **7**, 011017 (2017).
- [18] C. W. Glass, A. R. Oganov, and N. Hansen, Uspex—evolutionary crystal structure prediction, *Computer Physics Communications* **175**, 713 (2006).
- [19] A. R. Oganov, *Modern methods of crystal structure prediction* (John Wiley & Sons, 2011).
- [20] Y. Wang, J. Lv, L. Zhu, and Y. Ma, Calypso: A method for crystal structure prediction, *Computer Physics Communications* **183**, 2063 (2012).
- [21] Y. Wang and Y. Ma, Perspective: Crystal structure

- prediction at high pressures, *The Journal of Chemical Physics* **140**, 040901 (2014).
- [22] T. Yamashita, S. Kanehira, N. Sato, H. Kino, K. Terayama, H. Sawahata, T. Sato, F. Utsuno, K. Tsuda, T. Miyake, and T. Oguchi, Cryspy: a crystal structure prediction tool accelerated by machine learning, *Science and Technology of Advanced Materials: Methods* **1**, 87 (2021).
- [23] T. Kadowaki and H. Nishimori, Quantum annealing in the transverse Ising model, *Phys. Rev. E* **58**, 5355 (1998).
- [24] C. Durr and P. Hoyer, A quantum algorithm for finding the minimum (1999), [arXiv:quant-ph/9607014](https://arxiv.org/abs/quant-ph/9607014) [quant-ph].
- [25] S. Tanaka, R. Tamura, and B. K. Chakrabarti, *Quantum spin glasses, annealing and computation* (Cambridge University Press, 2017).
- [26] T. Albash and D. A. Lidar, Adiabatic quantum computation, *Rev. Mod. Phys.* **90**, 015002 (2018).
- [27] T. Jones, S. Endo, S. McArdle, X. Yuan, and S. C. Benjamin, Variational quantum algorithms for discovering hamiltonian spectra, *Phys. Rev. A* **99**, 062304 (2019).
- [28] S. McArdle, T. Jones, S. Endo, Y. Li, S. C. Benjamin, and X. Yuan, Variational ansatz-based quantum simulation of imaginary time evolution, *npj Quantum Information* **5**, 75 (2019).
- [29] T. Kosugi, Y. Nishiya, H. Nishi, and Y. Matsushita, Imaginary-time evolution using forward and backward real-time evolution with a single ancilla: First-quantized eigensolver algorithm for quantum chemistry, *Phys. Rev. Res.* **4**, 033121 (2022).
- [30] V. S. Denchev, S. Boixo, S. V. Isakov, N. Ding, R. Babbush, V. Smelyanskiy, J. Martinis, and H. Neven, What is the computational value of finite-range tunneling?, *Phys. Rev. X* **6**, 031015 (2016).
- [31] M. A. Nielsen and I. L. Chuang, Quantum computation and quantum information, *Phys. Today* **54**, 60 (2001).
- [32] P. Hauke, H. G. Katzgraber, W. Lechner, H. Nishimori, and W. D. Oliver, Perspectives of quantum annealing: methods and implementations, *Reports on Progress in Physics* **83**, 054401 (2020).
- [33] A. D. King, S. Suzuki, J. Raymond, A. Zucca, T. Lanting, F. Altomare, A. J. Berkley, S. Ejtemaee, E. Hoskinson, S. Huang, E. Ladizinsky, A. J. R. MacDonald, G. Marsden, T. Oh, G. Poulin-Lamarre, M. Reis, C. Rich, Y. Sato, J. D. Whittaker, J. Yao, R. Harris, D. A. Lidar, H. Nishimori, and M. H. Amin, Coherent quantum annealing in a programmable 2,000 qubit Ising chain, *Nature Physics* **18**, 1324 (2022).
- [34] C. C. McGeoch, R. Harris, S. P. Reinhardt, and P. I. Bunyk, Practical annealing-based quantum computing, *Computer* **52**, 38 (2019).
- [35] K. Boothby, P. Bunyk, J. Raymond, and A. Roy, Next-generation topology of D-Wave quantum processors (2020), [arXiv:2003.00133](https://arxiv.org/abs/2003.00133) [quant-ph].
- [36] H. Hirai, T. Horiba, S. Shirai, K. Kanno, K. Omiya, Y. O. Nakagawa, and S. Koh, Molecular structure optimization based on electrons–nuclei quantum dynamics computation, *ACS Omega* **7**, 19784 (2022).
- [37] T. Kosugi, H. Nishi, and Y.-i. Matsushita, Exhaustive search for optimal molecular geometries using imaginary-time evolution on a quantum computer, *npj Quantum Information* **9**, 112 (2023).
- [38] Y. Nishiya, H. Nishi, Y. Couzinié, T. Kosugi, and Y.-i. Matsushita, First-quantized adiabatic time evolution for the ground state of a many-electron system and the optimal nuclear configuration, *Phys. Rev. A* **109**, 022423 (2024).
- [39] V. V. Gusev, D. Adamson, A. Deligkas, D. Antypov, C. M. Collins, P. Krysta, I. Potapov, G. R. Darling, M. S. Dyer, P. Spirakis, and M. J. Rosseinsky, Optimality guarantees for crystal structure prediction, *Nature* **619**, 68 (2023).
- [40] Y. Couzinié, Y. Nishiya, H. Nishi, T. Kosugi, H. Nishimori, and Y.-i. Matsushita, Annealing for prediction of grand canonical crystal structures: Implementation of n -body atomic interactions, *Phys. Rev. A* **109**, 032416 (2024).
- [41] K. Ichikawa, S. Ohuchi, K. Ueno, and T. Yokoyama, Accelerating optimal elemental configuration search in crystal using Ising machine (2023), [arXiv:2305.19625](https://arxiv.org/abs/2305.19625) [cond-mat.mtrl-sci].
- [42] K. Nawa, T. Suzuki, K. Masuda, S. Tanaka, and Y. Miura, Quantum annealing optimization method for the design of barrier materials in magnetic tunnel junctions, *Phys. Rev. Appl.* **20**, 024044 (2023).
- [43] H. Sampei, K. Saegusa, K. Chishima, T. Higo, S. Tanaka, Y. Yayama, M. Nakamura, K. Kimura, and Y. Sekine, Quantum annealing boosts prediction of multimolecular adsorption on solid surfaces avoiding combinatorial explosion, *JACS Au* **3**, 991 (2023).
- [44] J. Tersoff, New empirical approach for the structure and energy of covalent systems, *Phys. Rev. B* **37**, 6991 (1988).
- [45] M. W. Finnis and J. E. Sinclair, A simple empirical n -body potential for transition metals, *Philosophical Magazine A* **50**, 45 (1984), <https://doi.org/10.1080/01418618408244210>.
- [46] V. Botu, R. Batra, J. Chapman, and R. Ramprasad, Machine learning force fields: Construction, validation, and outlook, *The Journal of Physical Chemistry C* **121**, 511 (2017).
- [47] M. S. Daw and M. I. Baskes, Embedded-atom method: Derivation and application to impurities, surfaces, and other defects in metals, *Phys. Rev. B* **29**, 6443 (1984).
- [48] B.-J. Lee, W.-S. Ko, H.-K. Kim, and E.-H. Kim, The modified embedded-atom method interatomic potentials and recent progress in atomistic simulations, *Calphad* **34**, 510 (2010).
- [49] N. Mohseni, P. L. McMahon, and T. Byrnes, Ising machines as hardware solvers of combinatorial optimization problems, *Nature Reviews Physics* **4**, 363 (2022).
- [50] M. Aramon, G. Rosenberg, E. Valiante, T. Miyazawa, H. Tamura, and H. G. Katzgraber, Physics-inspired optimization for quadratic unconstrained problems using a digital annealer, *Frontiers in Physics* **7**, 10.3389/fphy.2019.00048 (2019).
- [51] E. Farhi, J. Goldstone, and S. Gutmann, A quantum approximate optimization algorithm (2014), [arXiv:1411.4028](https://arxiv.org/abs/1411.4028) [quant-ph].
- [52] T. Kanao and H. Goto, Simulated bifurcation for higher-order cost functions, *Applied Physics Express* **16**, 014501 (2022).
- [53] N. Dattani, Quadraticization in discrete optimization and quantum mechanics (2019), [arXiv:1901.04405](https://arxiv.org/abs/1901.04405) [quant-ph].
- [54] W. Kohn and L. J. Sham, Self-consistent equations including exchange and correlation effects, *Phys. Rev.* **140**, A1133 (1965).
- [55] K. Terayama, M. Sumita, R. Tamura, and K. Tsuda, Black-box optimization for automated discovery, *Ac-*

- counts of *Chemical Research* **54**, 1334 (2021).
- [56] K. Kitai, J. Guo, S. Ju, S. Tanaka, K. Tsuda, J. Shiomi, and R. Tamura, Designing metamaterials with quantum annealing and factorization machines, *Phys. Rev. Res.* **2**, 013319 (2020).
- [57] A. S. Koshikawa, M. Ohzeki, T. Kadowaki, and K. Tanaka, Benchmark test of black-box optimization using d-wave quantum annealer, *Journal of the Physical Society of Japan* **90**, 064001 (2021), <https://doi.org/10.7566/JPSJ.90.064001>.
- [58] J. Nüßlein, C. Roch, T. Gabor, J. Stein, C. Linnhoff-Popien, and S. Feld, Black box optimization using qubo and the cross entropy method, in *Computational Science – ICCS 2023*, edited by J. Mikyska, C. de Mulatier, M. Paszynski, V. V. Krzhizhanovskaya, J. J. Dongarra, and P. M. Sloot (Springer Nature Switzerland, Cham, 2023) pp. 48–55.
- [59] L. Schmid, E. Zardini, and D. Pastorello, A general learning scheme for classical and quantum Ising machines (2023), [arXiv:2310.18411 \[cs.LG\]](https://arxiv.org/abs/2310.18411).
- [60] S. Izawa, K. Kitai, S. Tanaka, R. Tamura, and K. Tsuda, Continuous black-box optimization with an Ising machine and random subspace coding, *Phys. Rev. Res.* **4**, 023062 (2022).
- [61] Y. Seki, R. Tamura, and S. Tanaka, Black-box optimization for integer-variable problems using Ising machines and factorization machines (2022), [arXiv:2209.01016 \[cs.LG\]](https://arxiv.org/abs/2209.01016).
- [62] J. Thomas, Failure of the cauchy relation in cubic metals, *Scripta Metallurgica* **5**, 787 (1971).
- [63] M. S. Daw, S. M. Foiles, and M. I. Baskes, The embedded-atom method: a review of theory and applications, *Materials Science Reports* **9**, 251 (1993).
- [64] S. Rendle, Factorization machines, in *2010 IEEE International Conference on Data Mining* (2010) pp. 995–1000.
- [65] D. Bertsimas and J. Tsitsiklis, Simulated Annealing, *Statistical Science* **8**, 10 (1993).
- [66] A. Hjorth Larsen, J. Jørgen Mortensen, J. Blomqvist, I. E. Castelli, R. Christensen, M. Dulak, J. Friis, M. N. Groves, B. Hammer, C. Hargus, E. D. Hermes, P. C. Jennings, P. Bjerre Jensen, J. Kermodé, J. R. Kitchin, E. Leonhard Kolsbjerg, J. Kubal, K. Kaasbjerg, S. Lysgaard, J. Bergmann Maronsson, T. Maxson, T. Olsen, L. Pastewka, A. Peterson, C. Rostgaard, J. Schiøtz, O. Schütt, M. Strange, K. S. Thygesen, T. Vegge, L. Vilhelmsen, M. Walter, Z. Zeng, and K. W. Jacobsen, The atomic simulation environment—a python library for working with atoms, *Journal of Physics: Condensed Matter* **29**, 273002 (2017).
- [67] E. B. Tadmor, R. S. Elliott, J. P. Sethna, R. E. Miller, and C. A. Becker, The potential of atomistic simulations and the Knowledgebase of Interatomic Models, *JOM* **63**, 17 (2011).
- [68] N. Bernardes, Theory of solid Ne, A, Kr, and Xe at 0K, *Physical Review* **112**, 1534 (1958).
- [69] R. S. Elliott and E. B. Tadmor, Knowledgebase of Interatomic Models (KIM) application programming interface (API), <https://openkim.org/kim-api> (2011).
- [70] E. Tadmor, Driver for the Lennard-Jones model uniformly shifted to have zero energy at the cutoff radius v004, OpenKIM, <https://doi.org/10.25950/bdff6a6> (2020).
- [71] E. Tadmor, Lennard-Jones model (shifted) for Kr with parameters from Bernardes (1958) (low precision cutoff) v004, OpenKIM, <https://doi.org/10.25950/29c4bf9b> (2020).
- [72] F. H. Stillinger and T. A. Weber, Computer simulation of local order in condensed phases of silicon, *Physical Review B* **31**, 5262 (1985).
- [73] H. Balamane, T. Halicioglu, and W. A. Tiller, Vacancy- and adatom-induced $\sqrt{3} \times \sqrt{3}$ reconstructions of the Si(111) surface, *Physical Review B* **40**, 9999 (1989).
- [74] H. Balamane, T. Halicioglu, and W. A. Tiller, Comparative study of silicon empirical interatomic potentials, *Physical Review B* **46**, 2250 (1992).
- [75] A. K. Singh, H. Balamane, T. Halicioglu, and W. A. Tiller, Stillinger-Weber potential for Si developed by Balamane, Halicioglu and Tiller (1992) v005, OpenKIM, <https://doi.org/10.25950/3dc2cb7f> (2021).
- [76] M. Wen, Y. Afshar, F. H. Stillinger, and T. A. Weber, Stillinger-Weber (SW) Model Driver v005, OpenKIM, <https://doi.org/10.25950/934dca3e> (2021).
- [77] Y. Afshar, S. Hütter, R. E. Rudd, A. Stukowski, W. W. Tipton, D. R. Trinkle, G. J. Wagner, P. Zhang, E. Alonso, M. I. Baskes, V. V. Bulatov, T. D. de la Rubia, J. Kim, J. D. Kress, B.-J. Lee, T. Lenosky, J. S. Nelson, B. Sadigh, A. F. Voter, and A. F. Wright, The modified embedded atom method (MEAM) potential v002, OpenKIM, <https://doi.org/10.25950/ee5eba52> (2023).
- [78] B.-J. Lee, J.-H. Shim, and H. M. Park, A semi-empirical atomic potential for the Fe-Cr binary system, *Calphad* **25**, 527 (2001).
- [79] B.-J. Lee, J.-H. Shim, and H. M. Park, MEAM Potential for the Fe-Cr system developed by Lee, Shim and Park (2001) v001, OpenKIM, <https://doi.org/10.25950/8ce938a3> (2023).
- [80] A. Jain, S. P. Ong, G. Hautier, W. Chen, W. D. Richards, S. Dacek, S. Cholia, D. Gunter, D. Skinner, G. Ceder, and K. A. Persson, Commentary: The Materials Project: A materials genome approach to accelerating materials innovation, *APL Materials* **1**, 011002 (2013).
- [81] Data retrieved from the Materials Project for CrFe (mp-1226211) from database version v2023.11.1.
- [82] M. G. Kendall, A new measure of rank correlation, *Biometrika* **30**, 81 (1938).
- [83] S. Rendle, Factorization machines with libfm, *ACM Trans. Intell. Syst. Technol.* **3**, 10.1145/2168752.2168771 (2012).
- [84] M. Blondel, A. Fujino, N. Ueda, and M. Ishihata, Higher-order factorization machines, *Advances in Neural Information Processing Systems* **29** (2016).
- [85] A. Glielmo, P. Sollich, and A. De Vita, Accurate interatomic force fields via machine learning with covariant kernels, *Phys. Rev. B* **95**, 214302 (2017).
- [86] J. Vandermause, S. B. Torrisi, S. Batzner, Y. Xie, L. Sun, A. M. Kolpak, and B. Kozinsky, On-the-fly active learning of interpretable bayesian force fields for atomistic rare events, *npj Computational Materials* **6**, 20 (2020).
- [87] C. Bishop, Pattern recognition and machine learning, Springer google schola **2**, 531 (2006).